Modeling the Evolution and Life Cycle of Stable Cold Pools

TRAVIS H. WILSON AND ROBERT G. FOVELL

Department of Atmospheric and Oceanic Sciences, University of California, Los Angeles,
Los Angeles, California

ABSTRACT

Stable cold pools in California's Central Valley (CV) are conducive to freezing temperatures, high relative humidity, and, in some cases, fog. In this study it will be shown that the Weather Research and Forecasting (WRF) Model as commonly configured cannot reproduce such conditions because of a persistent warm and dry bias near the surface. It was found that removing horizontal diffusion, which by default operates on model levels and thus up and down the valley's sides, can reduce but not entirely fix the problem. Other improvements include enhancing the near-surface vertical resolution and the surface–air coupling, as both directly control the surface fluxes, especially evaporation. However, these alterations actually have the largest impact in the forested region surrounding the Central Valley, and influence the nighttime relative humidity in the CV only indirectly via nocturnal drainage flows. While it is not clear how realistic are the increased evaporation in the forest or the drainage flows, how and why these alterations result in significantly improved relative humidity reconstructions within the Central Valley are shown.

1. Introduction

Whiteman et al. (2001) defined a cold pool as a topographically confined, stagnant layer of air overlaid by warmer air aloft. Owing to its topography, cold pools develop frequently in the western United States. Cold pool conditions are conducive to fog formation, a dramatic and well-known example being the tule fog of California's heavily populated Central Valley (CV). If a cold pool lasts longer than one diurnal cycle, it is classified as persistent, whereas diurnal cold pools form at sunset and dissipate after sunrise (Whiteman et al. 2001).

In general, cold pools most commonly form during periods of high atmospheric pressure, light winds, and low solar insolation (Daly et al. 2009). As a result of their characteristic inversions, they can also assist in the formation of freezing rain, a hazard to transportation and safety (Whiteman et al. 2001). They also concentrate pollutants like ozone and fine particulates near the surface (Gillies et al. 2010; Baker et al. 2011), creating significant health hazards. Despite the impact they impose on air pollution and weather, however, persistent cold pools have received relatively little research attention (e.g., Zhong et al. 2001).

A common conceptual model concerning the formation of valley cold pools involves cold-air drainage after sunset as winds diminish and a shallow, stable boundary layer forms as a result of the strong radiative flux divergence. Negatively buoyant air originating on the side slopes of the valley descends to the stable layer, detaches from the sidewall, and flows out over the center of the basin (Clements et al. 2003). Essentially, the air above the valley center is efficiently cooled by the basin walls before becoming detached and this acts to enhance the cooling above the surface due to the sensible heat flux divergence (Whiteman et al. 1996). Further cooling in valleys is possible simply owing to their shape since a cross-sectional column of air over a valley is always smaller than that over flat terrain (Whiteman 2000), but this may be at least partially counteracted by downward longwave radiation originating from the atmosphere and valley walls in a manner that may be dependent on valley size (Whiteman et al. 2004).

However, the role of drainage flows in cold pool formation is controversial. In some cases, drainage flows do not become detached from the basin walls and have been well observed flowing in valley locations (Hootman and Blumen 1983; Gudiksen et al. 1992; Bodine et al. 2009). In other cases they are not even

Corresponding author address: Prof. Robert Fovell, Dept. of Atmospheric and Environmental Sciences, University at Albany, State University of New York, Albany, NY 12222.
E-mail: rfovell@albany.edu

observed or observable (Clements et al. 2003). In their analysis of 1997's Cooperative Atmospheric–Surface Exchange Study (CASES-97) field data, LeMone et al. (2003) attributed cold temperatures at low-elevation sites along Kansas' Walnut River to cold-air drainage and radiative cooling, but also found that the fast drainages observed at higher elevations were extremely weak lower down, leading the authors to suggest that the flows had become elevated over an even denser cold pool there. Indeed, Neff and King (1989) found that drainage flows in the Colorado River basin reside above a stronger surface-based inversion of lighter winds. Mahrt et al. (2001) examined CASES-99 observations in south-central Kansas and found that while the drainage flows do exist, their influence on the surface fluxes was undetectable owing to the limitations of their observing systems. Whiteman et al. (1996) also reported that the sensible heat flux at the valley floor they examined was nearly zero.

Some studies, including Thompson (1986), suggest that cold pool formation in open and closed valleys is a direct result of sheltering and not cold-air drainage. The presence of trees can reduce the vertical mixing that would otherwise bring warmer air down to the surface (Gustavsson et al. 1998). Basin size and terrain slope may play crucial roles (e.g., Katurji and Zhong 2012). In the gently sloping terrain of Oklahoma, Hunt et al. (2007) concluded that the cooling observed in cold pools occurred in situ, and Bodine et al. (2009) found that cold pools were suppressed by katabatic winds in the densely instrumented Lake Thunderbird Micronet. In fact, the latter went as far as stating that, "pooling of cold air as a result of drainage flow can clearly be excluded as a factor causing the CP [cold pool] development at the micronet." Instead, cold pool formation was likely caused by the cooling that occurred in situ as a result of the radiative heat loss and diminishing turbulent heat transfer in sheltered regions. (It should be noted that cooling aloft by drainage flows may indirectly assist in the in situ cooling at the surface by reducing the downward longwave radiation, though this effect may not be significant.)

However they are formed or maintained, failures to reproduce the development and persistence of cold pools and/or fogs have been reported for mesoscale numerical weather prediction models such as the Weather Research and Forecasting (WRF) Model's Advanced Research core (ARW; Skamarock et al. 2008), despite systematic improvements to the model physical parameterizations as well as the horizontal and vertical resolutions (e.g., Baker et al. 2011; Avery 2011; Ryerson 2012; Ryerson and Hacker 2014). Ryerson (2012) and Ryerson and Hacker (2014) found fog formation in the CV was prevented by a systematic warm
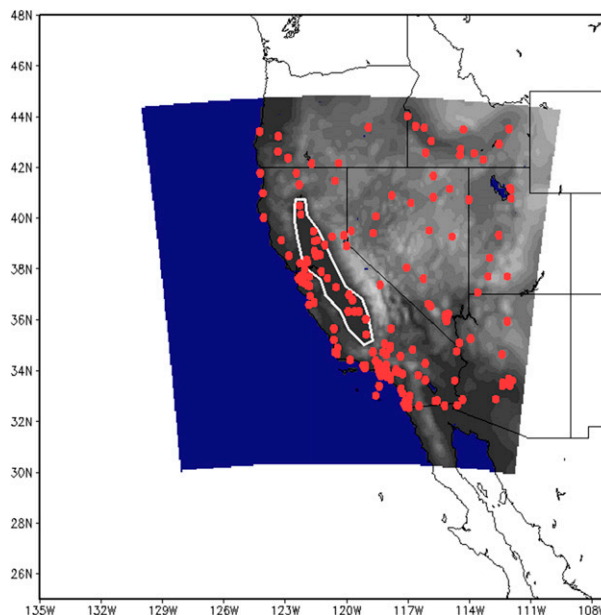
FIG. 1. The 36- (white) and 12-km (colored) domains used throughout all simulations in this article. The red dots represent surface ASOS or AWOS stations used to verify the model while the white polygon encloses stations used in the CV subset.

temperature bias during the overnight hours. Data assimilation and surface nudging have also been explored, with both failing to add value to the already poor representation of cold pools (e.g., Avery 2011). The cold pools that do develop often mix out too early, leading to erroneous surface temperatures and high pollutant concentrations (Avery 2011). It has been suggested that cold-pool-aware surface and/or boundary layer schemes are needed to accurately reproduce these stagnant air quality episodes (Baker et al. 2011; Avery 2011).

In this study, we explore cold pool development in California's CV using ARW and identify areas of improvement leading to superior reconstructions of nocturnal relative humidity, with an emphasis on how and why those changes were produced. The structure of this paper is as follows. Section 2 describes our methodology. Results are discussed in section 3, and in section 4 we present our concluding discussion.

2. Methodology

Our study employs ARW version 3.5, utilizing a nested-grid arrangement having horizontal resolutions of 36 and 12 km (Fig. 1) with 51 vertical levels. This numerical weather prediction model encompasses an enormous number of options, but many users are guided by provided examples and automatically selected options. By default (i.e., without specific user intervention),

TABLE 1. Default and shifted sigma levels used in WRF simulations, with corresponding scalar (half level) heights. Both use a total of 51 full vertical levels.

Model level	1	2	3	4	5	6	7
Default sigma values (full levels)	0.993	0.983	0.970	0.954	0.934	0.909	0.880
Default scalar heights (m AGL)	27	92	181	294	437	618	840
Shifted levels (full levels)	0.997	0.986	0.972	0.955	0.935	0.909	0.880
Shifted scalar heights (m AGL)	13	68	162	281	428	615	843

the real-data WRF is designed to place seven levels in the lowest 1 km, with the lowest scalar height at about 27 m above ground level (AGL); see Table 1. Popular model physics selections for regional-scale simulations include the Yonsei University (YSU) planetary boundary layer (PBL) scheme (Hong et al. 2006), the Rapid Radiative Transfer Model (RRTM) longwave and Dudhia shortwave radiation parameterizations (Mlawer et al. 1997; Dudhia 1989), and the Noah land surface model (Chen et al. 1996) using the USGS land-use dataset. This combination, along with Purdue–Lin microphysics scheme (Lin et al. 1983) and horizontal diffusion computed on the terrain-influenced (sigma or σ) model surfaces (diff_opt = 1 in the namelist) will be referred to herein as the Default WRF.

We will show that this Default WRF configuration produces very poor reconstructions of relative humidity (RH) in California's Central Valley, yielding RH values that are far too low, especially at night. Enhancing horizontal resolution over the CV and surrounding areas (not shown) was generally not found to add significant value.[1] As the influence of the atmospheric initialization on this systematic RH underprediction was also found to be relatively minor, all atmospheric variables in this study are derived from the North American Regional Reanalysis (NARR). Additionally, all simulations presented herein utilize the YSU PBL and Noah land surface model (LSM). While these important physical parameterizations can impact the results, they by themselves do not fix the RH problem and adopting different schemes does not materially alter our findings or conclusions.

However, in contrast to the atmospheric data source, simulations were found to be somewhat sensitive to the soil initialization. Consequently, we have chosen to employ surface fields from a variety of sources including the NARR reanalysis itself, the North American Mesoscale Forecast System (NAM), the ECMWF interim reanalysis (ERA-Interim), and also from offline simulations spun up using NCAR's High Resolution Land Data Assimilation System (HRLDAS) with forcing from NASA's North American Land Data Assimilation System (NLDAS) (Mitchell et al. 2004; Xia et al. 2012) phase 2. These will be referred to as NARR, NARRnam, NARRera, and NARRspun, with the lower case letters (if present) reflecting the origin of the soil information used in the simulation. Here, "offline" simply refers to the fact that the LSM was forced using a previously created dataset (such as observations) and not a full-fledged numerical weather model.

The reason for using offline LSM simulations is to assure that surface and soil variables reach thermodynamic equilibrium prior to the time period of interest (e.g., Case et al. 2008). Since soil moisture has a rather long memory footprint (cf. Wu and Dickinson 2004), the past must be known in order to initialize a numerical model with correct present-day values. In this sense, it would be impossible to get realistic results without "spun soils," which is the reason why all soil datasets are spun up. However, it remains that various surface and subsurface datasets are created with different LSMs (or different versions), which creates potential inconsistencies.

The simulation period of interest is 4–16 December 2005, a mostly dry and stagnant interval conducive to cold pool formation. During this time, minimal precipitation fell from a weak front that made its way through the CV on 8 and 9 December. Model reconstructions will combine a sequence of shorter, overlapping 72-h simulations, in which a new run is initialized (as a cold start) every other day. This means the first 24 h of each segment overlaps the end of the previous simulation but is discarded. Offline HRLDAS simulations were initialized from the NAM model on 1 January 2004 and integrated through the end of our interest period.

Observation data were collected from the Meteorological Assimilation Data Ingest System (MADIS). Our principal focus is on the surface Automated Surface Observing System (ASOS) and Automated Weather Observing System (AWOS) stations (hereafter jointly referenced as ASOS), displayed as red dots in Fig. 1. As we are modeling cold pools in California's

---

[1] One of our improvements will be shown to be restricting horizontal diffusion on model levels, which can unrealistically mix air along mountain slopes. Enhancing resolution can mitigate this unrealistic mixing since it sharpens the terrain and reduces the spatial extent over which the along-slope mixing occurs.
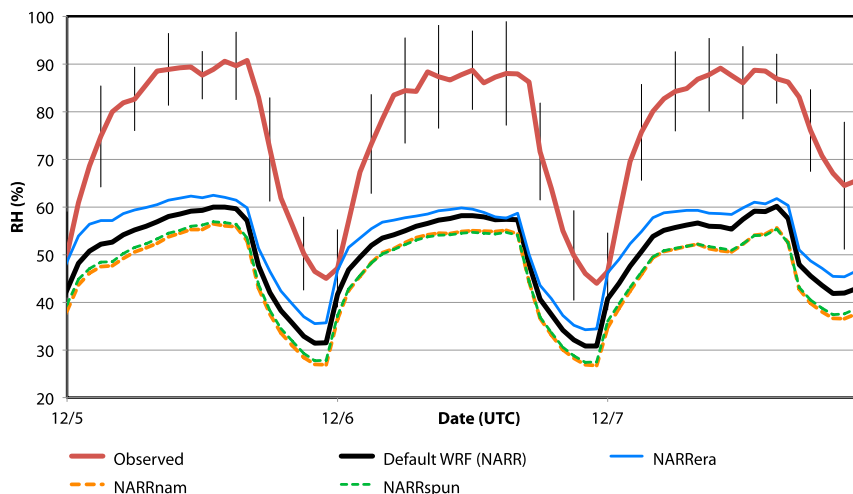
FIG. 2. Observed and modeled RH at 2 m AGL for the CV subset (Fig. 1) between 5 and 8 Dec. One standard deviation range around the mean observed RH is also shown. All simulations used the NARR atmospheric initialization with the Noah LSM and YSU PBL. Simulations labeled nam, spun, and era were initialized with NAM, HRLDAS, and ERA-Interim soils, respectively (see text).

CV, we will focus on statistics averaged over the stations within the white polygon, the "CV subset." Comparisons with observations were made using the Model Evaluation Tools (MET) software from the Developmental Testbed Center.

3. Results

Observed and modeled RH at 2 m AGL from 5 to 8 December for the CV subset can be seen in Fig. 2 with error bars representing plus or minus one standard deviation. Note that overnight relative humidity values were extremely moist—upward of 90%—during this period and the variation among the observations was quite small. In contrast, the RH diagnosed from the Default WRF simulation is several standard deviations too low, with an average bias during the period of −26% (see Table 2). Only slightly better, despite it being the best of these reconstructions, is the run that utilized ERA-Interim soil initialization (NARRera), while simulations using HRLDAS and NAM soil information (NARRspun and NARRnam) are quite comparable and not superior to the Default WRF.

It should be noted that (as revealed later) the large errors seen during this time interval are quite typical of the entire period of interest. Furthermore, reconstructions of comparable periods from different years yield very similar results. Additionally, we will soon demonstrate that this bias in relative humidity is a result of both overly warm overnight temperatures as well as predicted dewpoints that are too low, as suggested by Table 2.

a. Areas of improvement

Figure 2 shows that the Default WRF configuration is clearly incapable of properly forecasting near-surface conditions influencing relative humidity. We have identified three areas in which the WRF model can be altered to improve the creation and handling of cold pools in the Central Valley. We will see that each improvement, by itself, is insufficient to simulate observed conditions adequately, but the three in combination (the "cold pool configuration") results in acceptable model performance.

1) HORIZONTAL DIFFUSION

The WRF model handles subgrid-scale mixing in the vertical via the PBL scheme and in the horizontal via the diff_opt namelist option. Diffusion can be computed along model surfaces (diff_opt = 1), the default for real-data cases, or in physical space (diff_opt = 2). In the present situation, computing diffusion in physical space is desirable but can require rather high resolution to avoid instabilities associated with sharp terrain gradients. The default option, however, causes mixing up and down mountain slopes, which has been shown to be problematic in simulations of topographically confined cold pools (Billings et al. 2006; Zängl 2005). This is because adjacent grid points can vary dramatically in height, which in terms of cold pools means sizable differences in temperature, condensate, and water vapor.

Note that during the time period shown in Fig. 2, the average overnight (1200 UTC) RH in the CV was around 87%, while simulations with NARR- and

TABLE 2. Biases for the CV subset using different Noah/YSU WRF configurations during 6–8 Dec. These simulations were initialized with NARR atmospheric and soil datasets.

Configuration	RH bias (%)	Temp bias (K)	Dewpoint bias (K)
Default WRF	−25.62	1.72	−4.07
diffopt0	−17.74	0.88	−2.86
diffopt0 + shift	−14.76	0.33	−2.71
diffopt0 + IZ0	−11.40	0.32	−1.96
diffopt0 + shift + IZ0 (cold pool configuration)	−5.82	−0.21	−1.35
diffopt0 + shift + IZ0mod1	−11.94	0.04	−2.40
diffopt0 + shift + IZ0mod2	−12.85	0.34	−2.27

HRLDAS-initialized soils have relative humidities of only 58% and 54%, respectively (Fig. 2). Deactivating horizontal diffusion entirely (i.e., diff_opt = 0, abbreviated "diffopt0" herein) results in a substantial 11% increase in overnight relative humidity (not shown) and an 8% rise when averaged through the period (Table 2). By itself, this is a large improvement, but even these simulated RH values remain several standard deviations below the observed mean, so additional modifications need to be made.[2]

2) COUPLING STRENGTH

The "coupling strength" (Chen and Zhang 2009) is the amount of interaction permitted between the atmosphere and land surface, which among other factors is controlled by the exchange coefficient C_h, defined as

$$C_h = \frac{ku_*}{\ln\left(\frac{z_1}{z_{0T}}\right) - \psi_H}. \tag{1}$$

Here, k is the von Kármán constant, z_1 is the height of the first model level above the surface, z_{0T} is the so-called thermal roughness length, and ψ_H is the stability function for heat (Shin et al. 2012). This exchange coefficient, along with the vertical temperature–moisture gradient, directly controls the surface sensible and latent heat fluxes.

Chen and Zhang (2009) found that the Noah LSM underestimated values of C_h in forested regions while simultaneously overestimating it in more barren landscapes. To account for the changes in coupling strength owing to vegetation heights, they suggested

modifications to z_{0T} that improved simulations verified against data from the AmeriFlux network of sites providing automated and handmade measurements of ecosystem carbon, water, and energy fluxes. Simulations presented in this paper also ostensibly benefited from this option and will be discussed in depth presently. We will refer to this option as IZ0TLND, as it is referred to in the WRF namelist, and abbreviate it to IZ0.

3) SHIFTED LEVELS

The third area of improvement focuses on the height of the lowest model level for horizontal wind and scalars. By default, the WRF real.exe program fixes this level at $\sigma = 0.993$, which is approximately 27 m above the surface, independent of the number of vertical levels requested. For some simulations, the lowest sigma value is altered to $\sigma = 0.997$, which is approximately 13 m AGL. In those runs, the next four model levels are also shifted downward so there is no large change in resolution (see Table 1). This acts to increase the resolution at the surface while decreasing it—albeit only slightly—farther aloft as no additional levels are added. Among other things, this modification, which will sometimes be referred to as shift or shifted levels, causes a change in the energy balance, as discussed below.

b. Results with improvements

Figure 3 presents time series between 6 and 8 December of 2-m temperature and dewpoint[3] for the Default WRF configuration (black curves), as well as simulations employing combinations of our three identified improvements. With the Default WRF, the temperature is consistently too high and the dewpoint too low, especially during the overnight hours, resulting in the substantial negative RH bias noted previously (see also Table 2). By simply turning off diffusion along model levels (diffopt0), the temperature is lowered and the dewpoint is raised, partially mitigating the humidity underprediction. Evidently, mixing along model levels forces warmer and drier air down the slopes into the CV, but Fig. 3 reinforces our earlier point that this single alteration is insufficient. Shifting the lowest model levels closer to the surface (diffopt0 + shift) has a further, if rather modest, benefit (not shown).

---

[2] Partly as a consequence of this research, the diff_opt = 2 option has been modified in the WRF model to restrict mixing where terrain gradients are large. While this helps avoid the instabilities noted above, we have found the results with this new version to be immaterially different from those neglecting horizontal mixing entirely (diff_opt = 0).

[3] The spike in modeled dewpoints seen around sunset (7 December) appears to be a diagnostics issue and does not appear in the first model level dewpoints. The precise explanation for this is unknown.
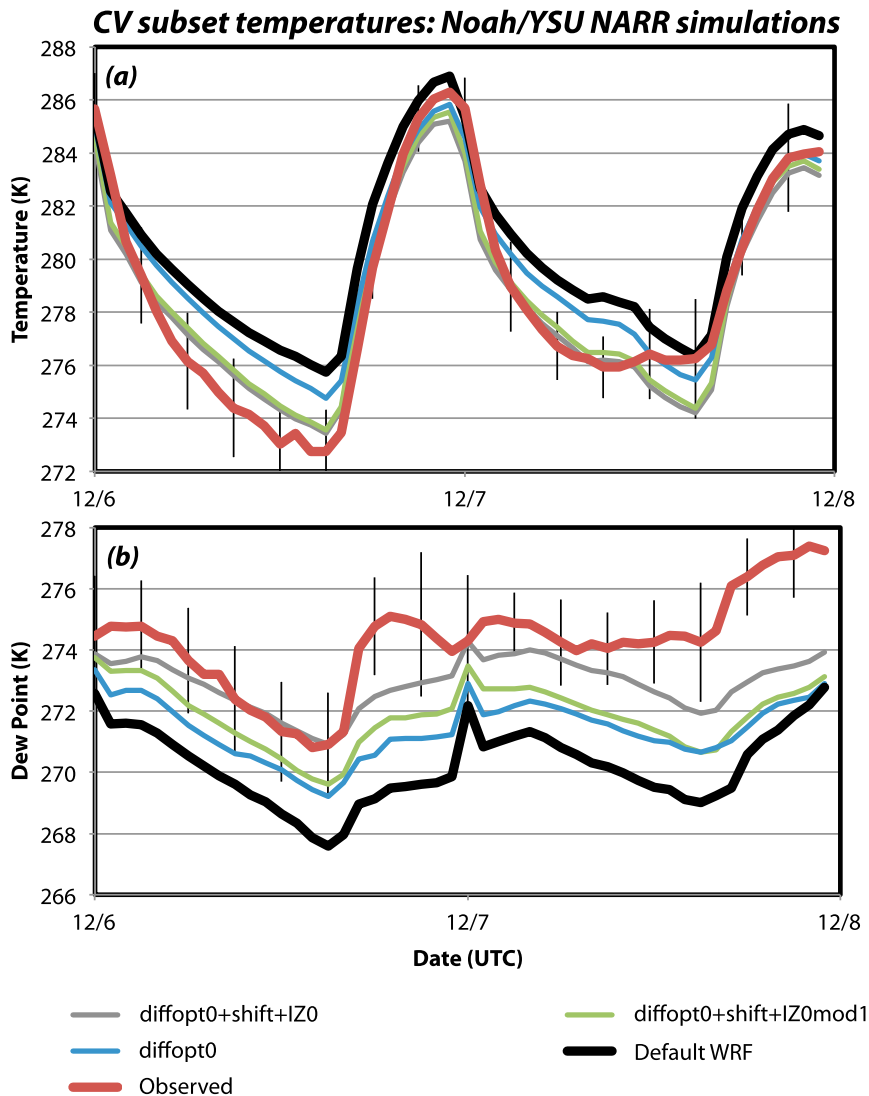
FIG. 3. Observed and modeled 2-m (a) temperatures and (b) dewpoints between 6 and 8 Dec for the CV subset. One standard deviation range around the mean observed value is also shown.

Implementing all three improvements (diffopt0 + shift + IZ0, gray curve) results in an even better reconstruction. This cold pool configuration has virtually no overnight minimum temperature (1500 UTC) bias (only 0.1 K) when averaged over the entire simulation period, 4–16 December (not shown), a substantial skill enhancement over the Default WRF, which had overnight minima that were, on average, 2.4 K too warm. Dewpoints are also generally better forecast although they are still negatively biased (see also Table 2). This underprediction can be partially mitigated by replacing the NARR's soil moisture with the ERA-Interim's initialization, as already suggested by Fig. 2 and further demonstrated below.

It is intuitively reasonable that, other factors being equal, increasing soil moisture in the topmost layer (10 cm thick in the Noah LSM) can encourage higher near-surface dewpoints. Soil moistures in this layer do vary dramatically among the different soil initializations employed in this study and are illustrated in Fig. 4a, which reports volumetric soil moisture values at the Central Valley's 21 surface stations, averaged through the 4–16 December period and ordered by latitude. While soil moisture is generally higher in the northern part of the CV in all cases, note that the driest source (NAM, labeled NARRnam) at its most moist location (north of 39°N) has a soil moisture that is comparable to the wettest source (ERA-Interim, labeled NARRera)
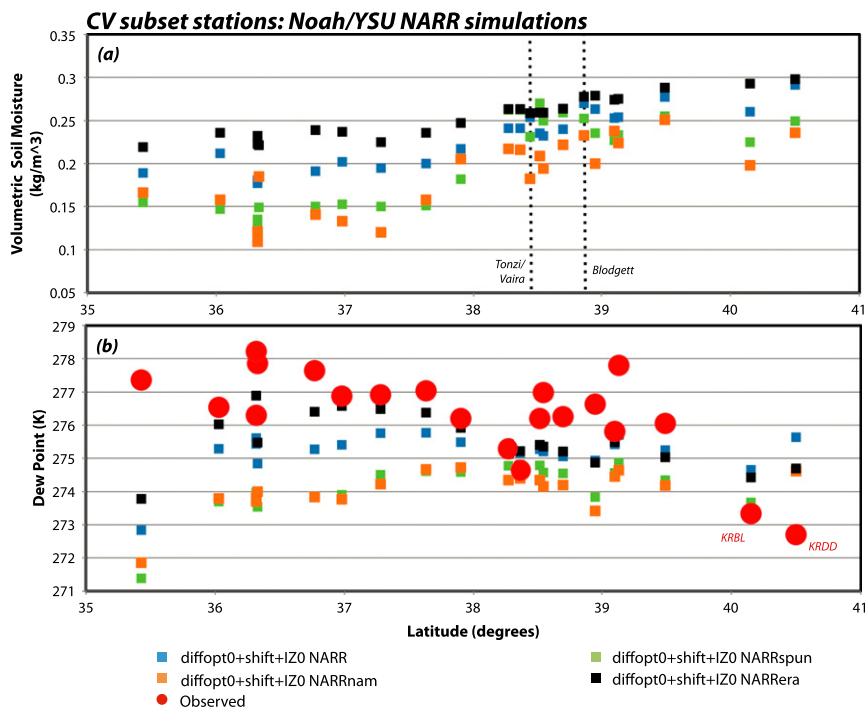
FIG. 4. Average values for (a) top-layer (0–10 cm) soil moisture values and (b) 2-m dewpoints between 4 and 16 Dec for the 21 ASOS stations in the CV ordered by latitude. The vertical black dashed lines represent the latitudes of (and soil moistures for) the Tonzi Ranch and Vaira Ranch (38.4°N) and the Blodgett Forest (38.9°N) AmeriFlux sites.

where it is driest (at the CV's southern end). These discrepancies are disconcerting because true soil moisture values are not known.

Furthermore, note that the soil moisture variation is particularly large in the San Joaquin Valley (the portion of the CV at and south of 38°N) where larger water contents are clearly associated with higher period-averaged dewpoints (Fig. 4b). Although markedly improved from the Default WRF configuration (not shown; but see Figs. 2 and 3), these modeled dewpoints are derived from simulations employing all identified improvements (shifted levels, IZ0TLND, and preventing horizontal diffusion on model levels) and are still negatively biased nearly everywhere.[4] This might suggest that the top-level soils remain too dry in the CV, even in the wettest soil source (ERA-Interim). The analysis below, however, leads to a somewhat different conclusion.

---

[4] At the two northernmost stations, Redding (KRDD) and Red Bluff (KRBL), the simulated dewpoints were similar to those for the rest of the valley but positively biased relative to the observations. These stations experience localized downslope winds during winter that are more effective in mixing dry air down to the surface in reality than in our simulations.

c. How remote evaporation influences Central Valley humidity

Figure 2 has already suggested that soil moisture is insufficient by itself to eradicate the persistent humidity bias in the Default WRF configuration, especially during the sunless hours. The IZ0TLND option can act to enhance surface evaporation from a given reservoir of soil moisture. However, Fig. 5a demonstrates that IZ0TLND does not actually alter evaporation in the CV significantly, although it increases it in the surrounding mountains. Shown is the latent heat flux difference between simulations made with and without IZ0TLND, both already neglecting horizontal diffusion along model surfaces (i.e., diffopt0), averaged over the period between 6 and 8 December. The most substantial latent heating enhancements occur in the forested areas represented by USGS land-use categories (LCs) 11–15, where the surface roughnesses are the largest (cf. with Fig. 6, which shows the spatial extent of the forest).

Evaporation can be further enhanced (albeit by a substantially smaller amount) in the mountains by also shifting the vertical levels closer to the surface, as illustrated in Fig. 5b. Thus, during this 48-h period one can see that the increase in evaporation from the run utilizing the IZ0TLND option is roughly $5–25\,\mathrm{W\,m^{-2}}$

Noah/YSU NARR simulations: 6-8 Dec latent heat flux differences
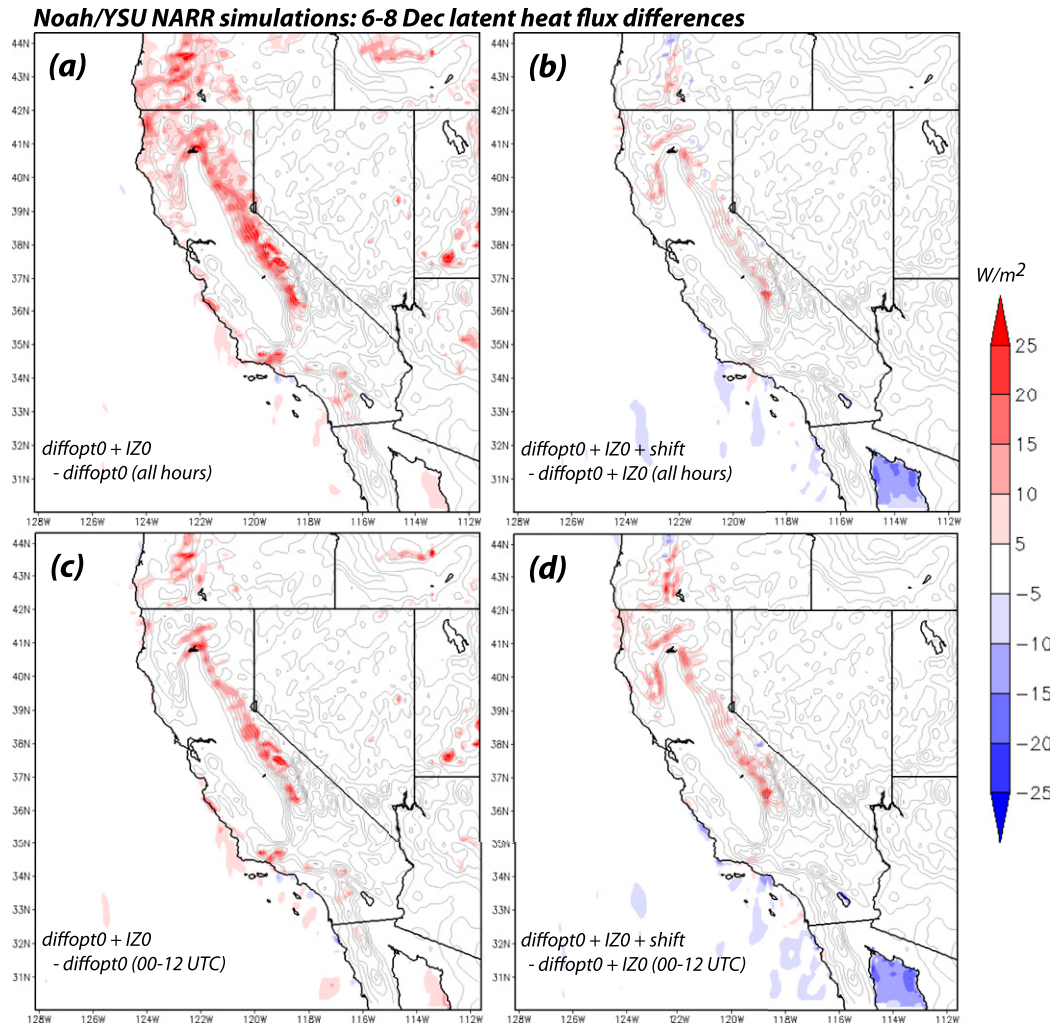
FIG. 5. Latent heat flux ($W\,m^{-2}$) differences (shaded) averaged between 6 and 8 Dec for Noah/YSU NARR simulations with (a) diffopt0 + IZ0 minus diffopt0 and (b) diffopt0 + IZ0 + shift minus diffopt0 + IZ0. (c),(d) As in (a),(b), respectively, but illustrating the differences restricted to overnight (0000–1200 UTC) hours. Terrain is contoured every 300 m.

higher in the surrounding terrain while altering the near-surface resolution further amplifies the flux there by approximately $5\,W\,m^{-2}$ at most. The evaporation alteration relative to the Default WRF in the CV remains insignificant, and this is due in part to persistent light wind conditions. It should be noted that while the simulations presented in Fig. 5 are initialized using NARR soils, enhanced evaporation rates brought about by IZ0TLND and shifted levels are also evident in the other soil initializations (not shown) as well.

To test whether the increase in dewpoints seen throughout the Central Valley is a direct result of the enhanced evaporation in the surrounding terrain, a modified version of the IZ0TLND option (IZ0mod1) is created that activates IZ0TLND everywhere except in

LCs 11–15, which includes the forested terrain that surrounds the CV. If the enhanced evaporation in the forested regions is indeed important, it would be reflected in the Central Valley dewpoints. Indeed, the CV dewpoints from this modified version (diffopt0 + shift + IZ0mod1; Fig. 3b) are only modestly improved from the shifted-levels run made without IZ0TLND (cf. Table 2), demonstrating that the CV dewpoints are heavily influenced by the increased evaporation from the surrounding forests. For surface temperatures (Fig. 3a), however, the modified version of the IZ0TLND option closely resembles the member utilizing all improvements. This means the increase in dewpoints is a nonlocal effect (involving the surrounding terrain) while the temperature decrease is local.
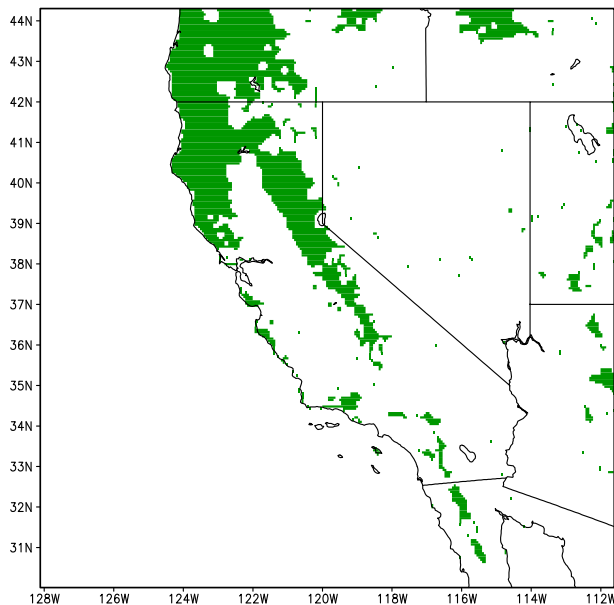
FIG. 6. Spatial extent of the forested area (green shaded area), representing LCs 11–15.

FIG. 7. Progress of a passive tracer initialized around sunset on 5 Dec 2005 in a Noah/YSU NARR simulation using the cold pool (diffopt0 + shift + IZ0) configuration. Colors depict regions having tracer concentrations exceeding 1/100th of the initial maximum value. Cross section is located at 38.55°N, and terrain is shaded in gray.

To recap, the Default WRF's average dewpoint bias through the period of 6–8 December is nearly −4.1 K (Table 2). By itself, preventing horizontal diffusion along model surfaces (diffopt0) reduces that dry bias by about 1.2 K. From this configuration, we see that altering the near-surface resolution and implementing IZ0TLND individually effect smaller (0.15 K) and larger (0.9 K) improvements, but these combine to reduce the dry bias by an even more substantial amount (1.5 K). Clearly, shifting the lowest model levels downward has a larger positive impact when IZ0TLND is also employed.

Furthermore, the magnitude of the improvement realized by combining IZ0TLND with shifted levels is larger than might be anticipated from Fig. 5b alone. To understand the outsized impact of the combination, one needs to inspect different hours of the day. Figures 5c and 5d are subsets of Figs. 5a and 5b, respectively, but are restricted to showing the latent heat flux change in the 0000–1200 UTC time period, which constitutes the bulk of the overnight hours. Comparison of Figs. 5a and 5c suggests that most of the impact of implementing the IZ0TLND option occurs during the day. (This is not surprising, as IZ0TLND enhances evaporation rates that naturally peak during the afternoon hours.) The opposite is true of the latent heat flux increase associated with shifted levels (Figs. 5b and 5d). When restricted to the overnight period, the enhancement contributed by altering the resolution is much more comparable to that owing to the IZ0TLND option itself.

Motivated by this, it was hypothesized that not only is evaporation from the forested region making a difference, but also it is the nighttime evaporation that has the larger influence. To test this explanation, another modified version (IZ0mod2) of IZ0TLND was created that activates the option everywhere except in LCs 11–14 between 0000 and 1200 UTC. This means the evaporation enhancement in the forest is permitted, but not during the bulk of the sunless period. This alteration improves the CV's negative dewpoint bias by a mere 0.13 K (to −2.27 K; see Table 2) from that found in the IZ0mod1 experiment, which enabled the IZ0TLND option everywhere except category 14. If the daytime evaporation were crucial, one would expect to see a much larger change in the dewpoint bias, as occurs with the cold pool (diffopt0 + shift + IZ0) configuration.

Thus, we have demonstrated that the increase in CV dewpoints is not only nonlocal but also essentially nocturnal. The reason for this is that the model simulations develop shallow drainage flows at night that are moistened by the IZ0TLND-enhanced evaporation. Figure 7 shows the path of a passive tracer in a simulation employing the cold pool configurations (diffopt0 + shift + IZ0). The tracer is introduced around sunset (labeled forecast hour 0) on the slope of the Sierra Nevada in an area where the IZ0TLND option has enhanced the surface latent heat flux. As the evening progresses, the tracer subsequently spreads down the slope and into the Central Valley, thereby illustrating a mechanism through which the

Noah/YSU NARR simulations: 6-8 December
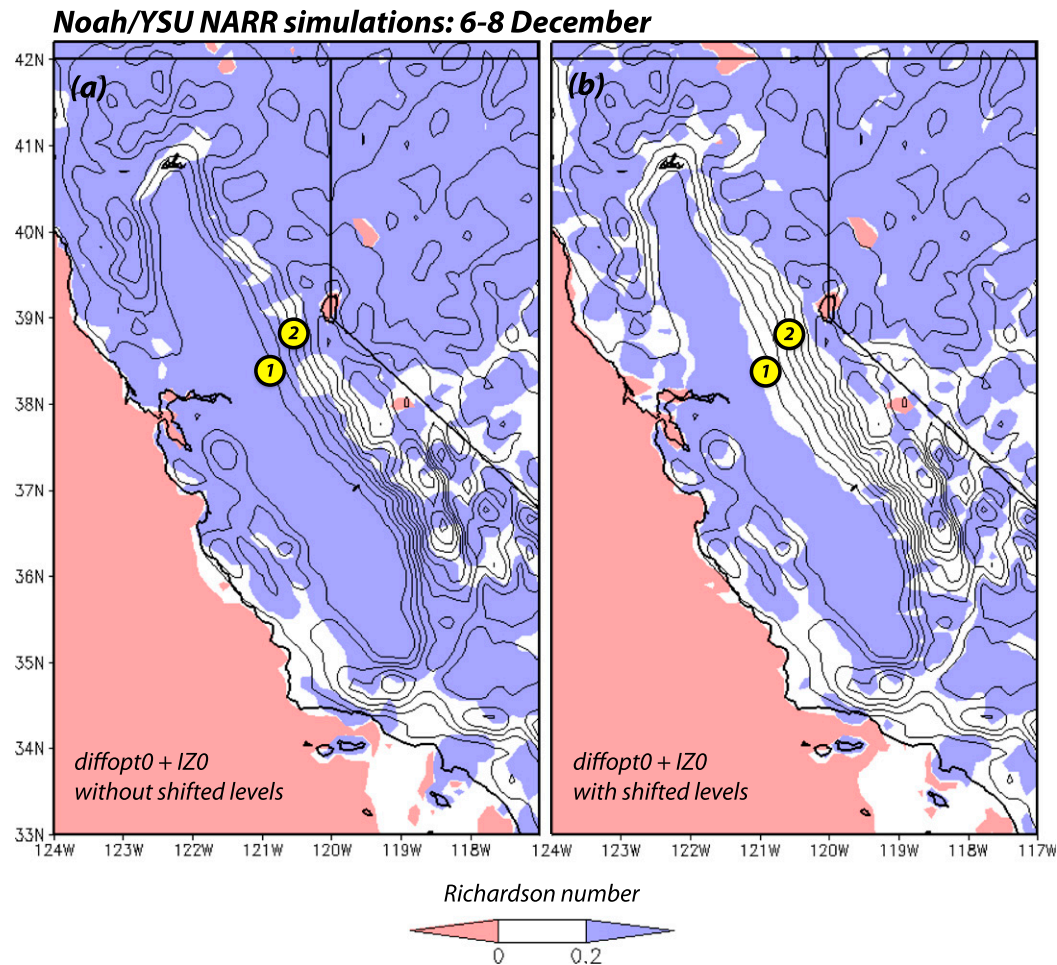
FIG. 8. Near-surface Richardson number averaged over 0300–1200 UTC between 6 and 8 Dec for simulations using the diffopt0 and IZ0 options (a) without and (b) with shifted levels. Terrain is contoured every 300 m and yellow dots indicate locations of the Tonzi and Vaira Ranches (CV sites collocated at dot 1) and the Blodgett Forest (Sierra site at dot 2) AmeriFlux stations.

surrounding forest can mitigate the Central Valley's negative dewpoint biases.

d. How near-surface vertical resolution influences Central Valley humidity

We have demonstrated that by shifting the lowest model levels down, the evaporation in the surrounding terrain increases, especially at night. However, why is evaporation sensitive to the height of the lowest model level in the first place? After all, the surface fluxes are dependent on the first model level's winds, which can be expected to become weaker as the lowest model level is shifted downward. Though not readily apparent, the enhanced evaporation does start with the winds on the lowest model level. Despite the fact that they are slower when that level is closer to the surface, the vertical shear actually increases, which has important

consequences for the bulk Richardson number (BRi), which is defined as

$$\text{BRi}(z) = \frac{\dfrac{g}{\theta}\dfrac{\partial\theta}{\partial z}}{\left(\dfrac{\partial U}{\partial z}\right)^2}, \qquad (2)$$

where g is the gravitational acceleration due to the earth's mass, θ is the potential temperature, z is height, and U is the total horizontal wind speed.

Figure 8 shows the BRi averaged over hours falling between 0300 and 1200 UTC, the middle of the nighttime period, for IZ0TLND simulations with and without shifting the model levels downward. Note that with the shift, a substantially larger portion of the foothills surrounding the Central Valley has an average BRi under
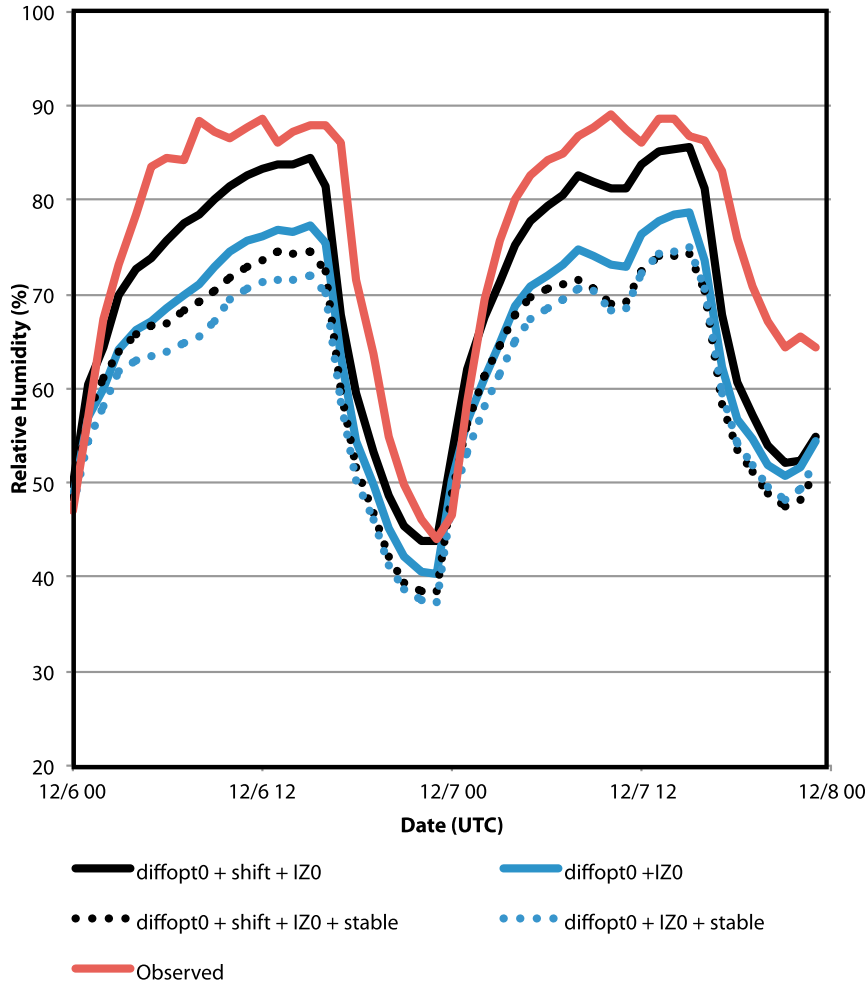
FIG. 9. Observed and modeled CV RH from 6 to 8 Dec for selected simulations with (solid) and without (dotted) using the mechanically damped turbulence regime.

0.2, which spatially coincides with where drainage flows and the enhanced evaporation from the IZ0TLND option are occurring. The Default WRF surface layer scheme uses BRi to determine the stability regime, which shifts from stable (BRi $\geq$ 0.2) to mechanically damped turbulence ($0 <$ BRi < 0.2) at this threshold value. The regime determines the magnitude of the stability function in (1) and, as one can imagine, shifting to a less stable regime would act to increase the exchange coefficient and the subsequent surface fluxes.

In the mechanically damped turbulence regime, the stability function ψ_H is reduced from its stable regime value by a factor depending on BRi. It was hypothesized that if ψ_H were not reduced in the mechanically damped turbulence regime, differences between simulations utilizing the default and shifted levels would effectively disappear. This was found to be true, as demonstrated in Fig. 9. Here, the relative humidity is shown for the CV

subset for simulations using the default and shifted levels, before (solid lines) and after (dotted lines) alteration of ψ_H. When the stability functions are not recomputed in the mechanically damped turbulence regime (dotted), the simulations are little different. This proves that shifting the levels acts to increase the resolved shear, decrease the Richardson number, change the regime, and finally alter the surface fluxes via the stability function.

e. Is the IZ0TLND evaporation enhancement realistic?

We have shown that a key element in mitigating the nocturnal CV dry bias is increasing evaporation in the surrounding forest during the nighttime hours via the IZ0TLND option. This section is concerned with the realism of the simulated evaporation rates, in the CV and the surrounding terrain, as we are leery of getting a
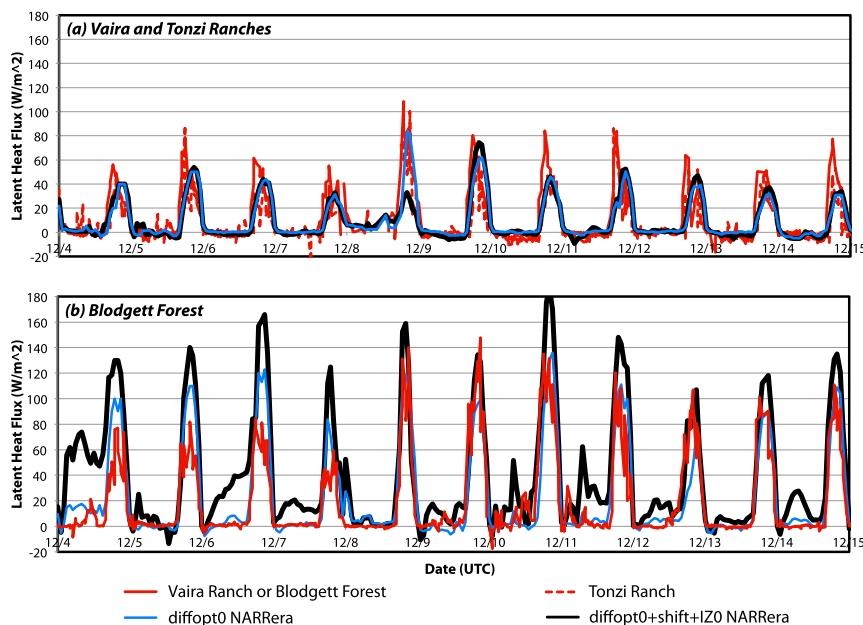
FIG. 10. Observed latent heat fluxes from 4 to 15 Dec at three AmeriFlux sites compared to Noah/YSU NARRera simulations. (a) The Vaira and Tonzi Ranches are located along the eastern edge of the CV and are approximately 3 km apart. (b) The Blodgett Forest site is located farther east in the Sierra Nevada and is in an evergreen needleleaf forest. See Fig. 8.

better simulation for the wrong reasons. It is important to tackle this problem but, regrettably, a clear answer does not emerge, so further research is needed.

A significant, practical issue is that observations of evaporation rates are scarce, especially during the period of interest, and can be expected to be profoundly influenced by local site characteristics. Nevertheless, Fig. 10 compares modeled latent heat fluxes to observations between 4 and 15 December at three AmeriFlux sites: Vaira Ranch and Tonzi Ranch, both located in the CV south and east of Sacramento, California, and Blodgett Forest in the Sierra Nevada evergreen needleleaf forest (see Fig. 8; Goldstein 2006). Simulations with and without both IZ0TLND and shifted levels are shown, with all runs employing the ERA-Interim (NARRera) soil initialization as that has the highest top-layer water content at nearly all CV ASOS stations as well as at the three AmeriFlux sites (see Fig. 4a) and thus the highest latent heat fluxes among the simulations. This source also results in the smallest dewpoint errors in the CV (Table 3).

The Tonzi and Vaira sites are represented by the same model grid point since they are roughly 3 km apart. However, they have different local land covers, which might explain why the observations do not agree consistently during the afternoon hours (Fig. 10a). Nevertheless, the NARRera-based simulated rates reside between the

observations on most days and the nocturnal fluxes appear realistic. Finally, one can observe that shifting the levels and activating IZ0TLND hardly affects the latent heat flux (except perhaps late on 8 December) in the CV, consistent with the results shown in Fig. 5.

That the IZ0TLND option most dramatically influences forested regions is again demonstrated in the Blodgett Forest (Fig. 10b) series. Here, the simulation with IZ0TLND and shifted levels appears to consistently overpredict evaporation rates, particularly during the critical nighttime hours. This raises the possibility that the IZ0TLND option is improving our simulations for an improper reason. However, one should keep in mind that the Blodgett Forest is the only AmeriFlux site surrounding the CV with data during this time period, that there may be many more reasons why evaporation is being overpredicted at this one particular point, and that it might not be representative of the high Sierra as a whole. As the amount of available data is extremely small, it would be very dangerous to extrapolate this result too far. Instead, it should be noted that we have demonstrated how and why the IZ0TLND option influences CV dewpoints and that it is much less direct and potentially more interesting than might initially be guessed.

In any event, to get a better understanding as to whether or not this increased evaporation is in fact

TABLE 3. Mean absolute error (MAE) and bias averaged over 4–16 Dec 2005 are shown for the Noah/YSU NARRera and Noah/YSU diffopt0 + shift+IZ0 NARRera simulations. There are approximately 20 verification points per hour in the CV and 144 in domain 2 (D2).

Verification region	Temp (K)		Dewpoint (K)		RH (%)	
	Bias	MAE	Bias	MAE	Bias	MAE
Noah/YSU NARRera						
CV	1.37	2.26	−2.21	2.77	−17.10	20.32
D2	0.75	2.63	−0.72	3.30	−6.63	15.11
Noah/YSU+shift+IZ0 + diffopt0 NARRera						
CV	−0.14	1.84	−0.63	1.76	−2.94	11.59
D2	−0.03	2.45	−0.17	3.05	−1.02	12.87

realistic, we examine dewpoint biases averaged through the 4–16 December period from NARRera simulations utilizing the diffopt0 (Figs. 11a,c) and diffopt0 + shift + IZ0 configurations (Figs. 11b,d) for hours that fall during the nighttime (1400 UTC, top row) and the daytime (2200 UTC, bottom row). The ASOS stations previously employed in our verification have been supplemented by Remote Automatic Weather Station (RAWS) sites to increase observation density (cf. to Fig. 1). Figure 11a shows that the overnight dry bias in the diffopt0-only version is prevalent not only in the CV but also across the surrounding terrain, which contrasts with the diffopt0 + shift + IZ0 configuration (Fig. 11b) that presents little net bias across the CV and surrounding terrain. This might suggest that the inflated evaporation rates produced by IZ0TLND in combination with shifted levels may be more realistic.

However, this point may be contradicted by the daytime dewpoint biases (Figs. 11c,d). One can see that the terrain surrounding the CV is nearly unbiased in the diffopt0-only version (Fig. 11c) while the shift + IZ0 + diffopt0 configuration (Fig. 11d) has a substantial net high dewpoint bias. This could indicate that the daytime evaporation rates are unrealistically large in the simulations using all improvements. That being said, it is the nighttime evaporation rates that truly matter for the CV dewpoints and, again, the evidence is neither complete nor unambiguous.

4. Summary and conclusions

Topographically confined cold pools pose a considerable forecasting and modeling challenge in many areas (Baker et al. 2011; Avery 2011), including California's heavily populated Central Valley (CV) that stretches from Redding in the north to Bakersfield in the south. When configured and initialized in a rather standard fashion, the WRF model yields erroneously low predictions of near-surface relative humidity (RH) in the CV during the wintertime. This has been encountered in a prior study (Ryerson 2012; Ryerson and Hacker 2014)

and is demonstrated in Fig. 12 for the CV subset over the entire 4–16 December 2005 period, with overlapping simulations initialized with NARR for the atmospheric variables and employing the YSU PBL and Noah land surface schemes. When the NARR's soil information is used (black dotted curve), the RH is clearly far too low relative to the observations (red curve), especially when weather conditions were dry and dominated by high pressure (e.g., between 5–8 and 10–13 December).

We found that replacing the NARR soils with wetter sources, such as from the ERA-Interim (resulting in simulation NARRera; blue curve in Fig. 12), results in only very modest improvements, while employing soils "spun up" in an offline model was determined to be unhelpful in this situation. In any event, note that the underpredictions remain particularly large during the night, when RH tends to be high and foggy conditions become more likely. We have demonstrated this is a consequence of both a warm bias in temperature and dewpoints that are too low during the sunless periods. Given the numerous travel corridors in the Central Valley and widespread occurrences of fog, this cannot go uncorrected.

Our analysis has highlighted several potential improvements in the model configuration, the first relating to horizontal diffusion. The recommended option with the real-data WRF is to perform this mixing along model surfaces that follow the terrain (i.e., namelist option diff_opt = 1), but we found this causes warm and dry air to be drawn down into the CV from the surrounding mountains. In theory, the solution is to have diffusion operate in physical space (diff_opt = 2) instead, but as of WRF version 3.6 this mixing is scaled by a nondimensional slope parameter that effectively shuts it off near sharply sloping terrain in order to maintain stability. As our simulations with diff_opt = 2 and deactivating horizontal diffusion altogether (diff_opt = 0, which we termed diffopt0) were nearly indistinguishable, we adopted the latter as part of our "cold pool configuration" (see section 3a), although the former would work just as well.
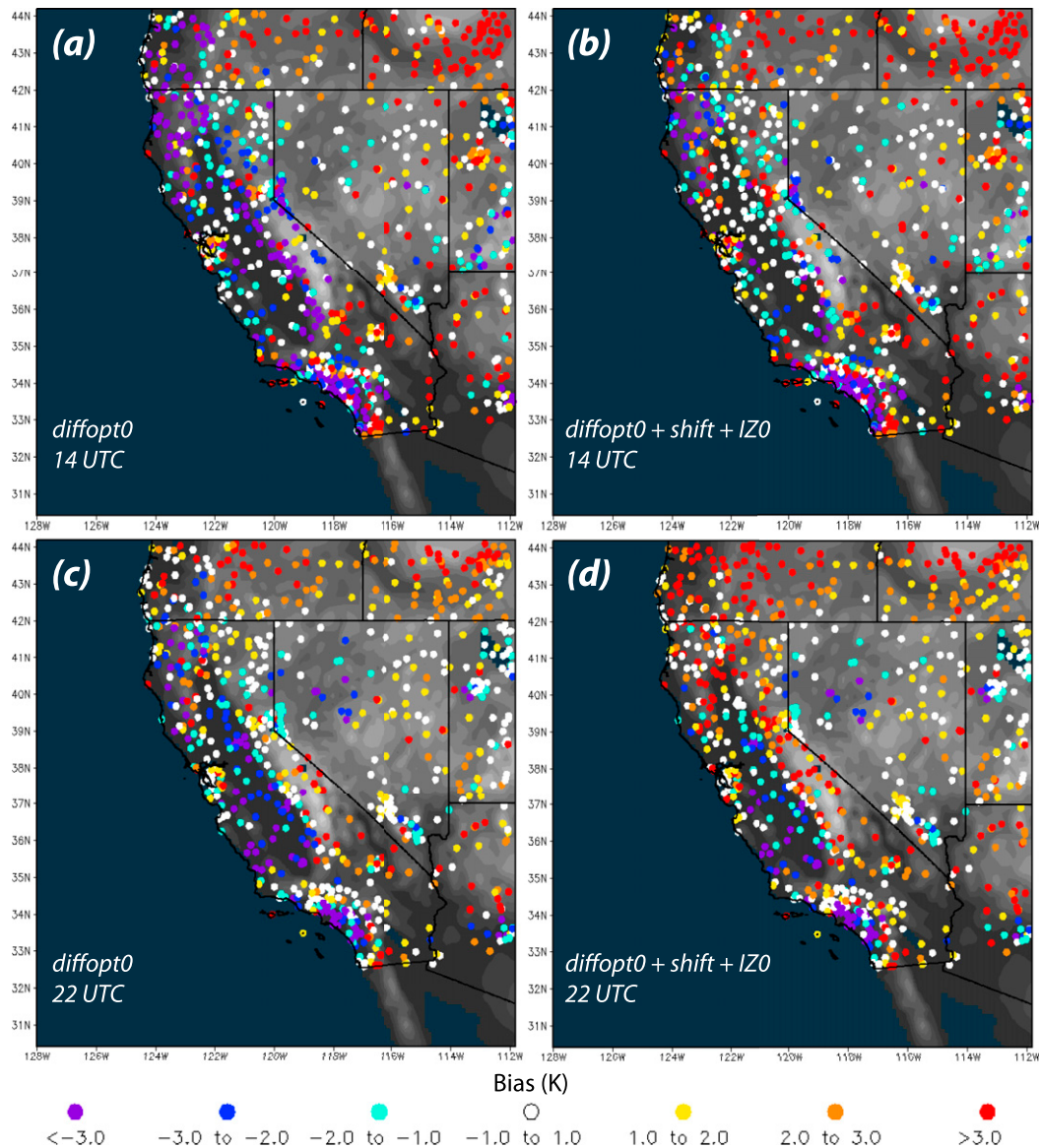
FIG. 11. Dewpoint bias (K) by station, averaged between 4 and 16 Dec, for Noah/YSU NARRera simulations with (a) diffopt0 only at 1400 UTC and (b) diffopt0 + shift + IZ0 at 1400 UTC. (c) As in (a), but at 2200 UTC. (d) As in (b), but at 2200 UTC. This figure incorporates ASOS and RAWS stations reporting for at least 10 of the period's 12 days.

With ERA-Interim soils, the diffopt0 modification to the Default WRF configuration results in higher but still unacceptably low RH values (gray curve in Fig. 12). When two additional modifications are implemented, however, CV RH predictions improve markedly. One is the Chen and Zhang (2009) thermal roughness length modification called IZ0TLND (and abbreviated IZ0) and the other is the enhancement of near-surface resolution by moving the lowest few model levels downward

(labeled shift). With these changes (solid black curve in Fig. 12), the pervasive nocturnal dry bias is nearly completely removed. It is important to note that on nights such as 13 and 14 December, when the Default WRF configuration's simulated relative humidity is relatively close to reality, the cold pool configuration version does not overpredict the low-level moisture, so we are not merely curing a negative bias at some times via introducing a positive one at other times.
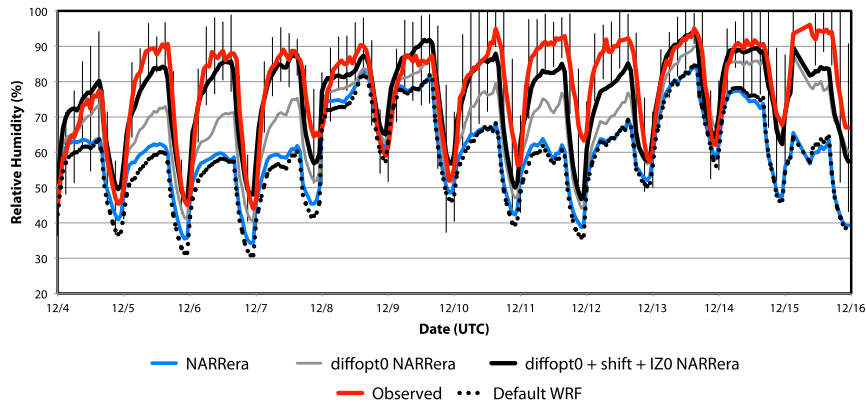
FIG. 12. Observed (red) and modeled RH for the CV subset from 4 to 16 Dec 2005, for Noah/YSU simulations with the Default WRF configuration using NARR (dotted black) and ERA-Interim (NARRera) soils (blue), as well as NARRera simulations using diffopt0 (dark gray) and all improvements (diffopt0 + shift + IZ0; solid black). Error bars depict plus or minus one standard deviation for observed RH every third hour.

The IZ0TLND option enhances evaporation from the surface and this leads to higher dewpoints in the CV. However, we found the evaporation that removes the CV dry bias occurs not in the valley itself but rather in the surrounding mountains and, furthermore, is dominated by nighttime evaporation when latent heating rates are typically not sizable. Even with IZ0TLND, evaporation in the CV remains small because the winds during the period of interest are fairly light. The IZ0TLND option induces higher latent heat fluxes at all hours, but the daytime increase in the surrounding forested terrain is of much less importance because there is no apparent mechanism to bring that moisture down to the CV's surface. In contrast, the IZ0TLND-enhanced evaporation at night is carried to the CV via nocturnal drainage flows, which we demonstrated to exist via passive tracers.

Activating the IZ0TLND option in the WRF model increases the coupling between the land and atmosphere in the surrounding forest because it directly modifies the thermal roughness length employed in the exchange coefficient C_h. In contrast, adjusting the height of the lowest model level impacts the nighttime evaporation owing to an indirect shift in the surface-layer scheme's stability function for heat ψ_H, which is controlled by the diagnosed stability regime. It was found that moving the lowest model level downward decreases the winds on the first model level almost everywhere, but enhances the surface-layer vertical shear in drainage-prone locations. As this increased shear lowers the Richardson number, it can change the diagnosed turbulence regime and thus the stability function, ultimately altering the surface fluxes (the latent heat flux in particular). Whether or not the shift

from the stable to the mechanically damped turbulence regime in the mountains where the drainage flows form is correct, this result serves to highlight how and why the simulations can be sensitive to the near-surface vertical resolution.

Finally, additional research is needed to verify that the larger surface fluxes observed in the simulations owing to the IZ0TLND option are actually realistic. At this point, the very limited evidence available suggests that the enhanced nocturnal evaporation rates produced by IZ0TLND are excessively high. It is possible that the elevated latent heat fluxes in the higher-elevation forest are essentially compensating for other model deficiencies, in the initialization and/or elsewhere in the model physics. One does not just want accurate forecasts; one also wants to get the right answers for the right reasons. This has to be left to future work.

REFERENCES

Avery, L., 2011: Challenges of meteorological and photochemical modeling of Utah's wintertime cold pools. *Proc. Western Meteorological, Emissions, and Air Quality Modeling Workshop*, Boulder, CO, Western Regional Air Partnership. [Available online at http://www.wrapair2.org/pdf/Avey_UT_ColdPolds.pdf.]

Baker, K. R., H. Simon, and J. T. Kelly, 2011: Challenges to modeling ''cold pool'' meteorology associated with high pollution episodes. *Environ. Sci. Technol.*, **45**, 7118–7119, doi:10.1021/es202705v.

Billings, B. J., V. Grubišić, and R. D. Borys, 2006: Maintenance of a mountain valley cold pool: A numerical study. *Mon. Wea. Rev.*, **134**, 2266–2278, doi:10.1175/MWR3180.1.

Bodine, D., P. M. Klein, S. C. Arms, and A. Shapiro, 2009: Variability of surface air temperature over gently sloped terrain. *J. Appl. Meteor. Climatol.*, **48**, 1117–1141, doi:10.1175/2009JAMC1933.1.

Case, J. L., W. L. Crosson, S. V. Kumar, W. M. Lapenta, and C. D. Peters-Lidard, 2008: Impacts of high-resolution land surface initialization on regional sensible weather forecasts from the WRF model. *J. Hydrometeor.*, **9**, 1249–1266, doi:10.1175/2008JHM990.1.

Chen, F., and Y. Zhang, 2009: On the coupling strength between the land surface and the atmosphere: From viewpoint of surface exchange coefficients. *Geophys. Res. Lett.*, **36**, L10404, doi:10.1029/2009GL037980.

——, and Coauthors, 1996: Modeling of land surface evaporation by four schemes and comparison with FIFE observations. *J. Geophys. Res.*, **101**, 7251–7268, doi:10.1029/95JD02165.

Clements, C. B., C. D. Whiteman, and J. D. Horel, 2003: Cold-air-pool structure and evolution in a mountain basin: Peter Sinks, Utah. *J. Appl. Meteor.*, **42**, 752–768, doi:10.1175/1520-0450(2003)042<0752:CSAEIA>2.0.CO;2.

Daly, C., D. Conklin, and M. Unsworth, 2009: Local atmospheric decoupling in complex topography alters climate change impacts. *Int. J. Climatol.*, **30**, 1857–1864, doi:10.1002/joc.2007.

Dudhia, J., 1989: Numerical study of convection observed during the Winter Monsoon Experiment using a mesoscale two-dimensional model. *J. Atmos. Sci.*, **46**, 3077–3107, doi:10.1175/1520-0469(1989)046<3077:NSOCOD>2.0.CO;2.

Gillies, R. R., S. Wang, and M. R. Booth, 2010: Atmospheric scale interaction on wintertime Intermountain West low-level inversions. *Wea. Forecasting*, **25**, 1196–1210, doi:10.1175/2010WAF2222380.1.

Goldstein, A., 2006: AmeriFlux US-Blo Blodgett Forest. Lawrence Berkeley National Laboratory, accessed November 2012, doi:10.17190/AMF/1246032.

Gudiksen, P. H., J. M. Leone Jr., C. W. King, D. Ruffieux, and W. D. Neff, 1992: Measurements and modeling of the effects of ambient meteorology on nocturnal drainage flows. *J. Appl. Meteor.*, **31**, 1023–1032, doi:10.1175/1520-0450(1992)031<1023:MAMOTE>2.0.CO;2.

Gustavsson, T., M. Karlsson, J. Bogren, and S. Lindqvist, 1998: Development of temperature patterns during clear nights. *J. Appl. Meteor.*, **37**, 559–571, doi:10.1175/1520-0450(1998)037<0559:DOTPDC>2.0.CO;2.

Hong, S.-Y., Y. Noh, and J. Dudhia, 2006: A new vertical diffusion package with an explicit treatment of entrainment processes. *Mon. Wea. Rev.*, **134**, 2318–2341, doi:10.1175/MWR3199.1.

Hootman, B. W., and W. Blumen, 1983: Analysis of nighttime drainage winds in Boulder, Colorado during 1980. *Mon. Wea. Rev.*, **111**, 1052–1061, doi:10.1175/1520-0493(1983)111<1052:AONDWI>2.0.CO;2.

Hunt, E. D., J. B. Basara, and C. R. Morgan, 2007: Significant inversions and rapid in situ cooling at a well-sited Oklahoma mesonet station. *J. Appl. Meteor. Climatol.*, **46**, 353–367, doi:10.1175/JAM2467.1.

Katurji, M., and S. Zhong, 2012: The influence of topography and ambient stability on the characteristics of cold-air pools: A numerical investigation. *J. Appl. Meteor. Climatol.*, **51**, 1740–1749, doi:10.1175/JAMC-D-11-0169.1.

LeMone, M. A., K. Ikeda, R. L. Grossman, and M. W. Rotach, 2003: Horizontal variability of 2-m temperature at night during CASES-97. *J. Atmos. Sci.*, **60**, 2431–2449, doi:10.1175/1520-0469(2003)060<2431:HVOMTA>2.0.CO;2.

Lin, Y.-L., R. D. Farley, and H. D. Orville, 1983: Bulk parameterization of the snow field in a cloud model. *J. Climate Appl. Meteor.*, **22**, 1065–1092, doi:10.1175/1520-0450(1983)022<1065:BPOTSF>2.0.CO;2.

Mahrt, L., D. Vickers, R. Nakamura, M. R. Soler, J. L. Sun, S. Burns, and D. H. Lenschow, 2001: Shallow drainage flows. *Bound.-Layer Meteor.*, **101**, 243–260, doi:10.1023/A:1019273314378.

Mitchell, K. E., and Coauthors, 2004: The multi-institution North American Land Data Assimilation System (NLDAS): Utilizing multiple GCIP products and partners in a continental distributed hydrological modeling system. *J. Geophys. Res.*, **109**, D07S90, doi:10.1029/2003JD003823.

Mlawer, E. J., S. J. Taubman, P. D. Brown, M. J. Iacono, and S. A. Clough, 1997: Radiative transfer for inhomogeneous atmospheres: RRTM, a validated correlated-k model for the longwave. *J. Geophys. Res.*, **102**, 16 663–16 682, doi:10.1029/97JD00237.

Neff, W. D., and C. W. King, 1989: The accumulation and pooling of drainage flows in a large basin. *J. Appl. Meteor.*, **28**, 518–529, doi:10.1175/1520-0450(1989)028<0518:TAAPOD>2.0.CO;2.

Ryerson, W. R., 2012: Toward improving short-range fog prediction in data-denied areas using the Air Force Weather Agency mesoscale ensemble. Ph.D. thesis, Naval Postgraduate School, Monterey, CA, 249 pp. [Available online at http://calhoun.nps.edu/bitstream/handle/10945/17454/12Sep_Ryerson_William_PhD.pdf?sequence=1.]

——, and J. P. Hacker, 2014: The potential for mesoscale visibility predictions with a multimodel ensemble. *Wea. Forecasting*, **29**, 543–562, doi:10.1175/WAF-D-13-00067.1.

Shin, H. H., S.-Y. Hong, and J. Dudhia, 2012: Impacts of the lowest model level height on the performance of planetary boundary layer parameterizations. *Mon. Wea. Rev.*, **140**, 664–682, doi:10.1175/MWR-D-11-00027.1.

Skamarock, W. C., and Coauthors, 2008: A description of the Advanced Research WRF version 3. NCAR Tech. Note NCAR/TN-475+STR, 113 pp., doi:10.5065/D68S4MVH.

Thompson, B. W., 1986: Small-scale katabatics and cold hollows. *Weather*, **41**, 146–153, doi:10.1002/j.1477-8696.1986.tb03813.x.

Whiteman, C. D., 2000: *Mountain Meteorology.* Oxford University Press, 355 pp.

——, T. B. McKee, and J. C. Doran, 1996: Boundary layer evolution within a canyonland basin. Part I: Mass, heat, and moisture budgets from observations. *J. Appl. Meteor.*, **35**, 2145–2161, doi:10.1175/1520-0450(1996)035<2145:BLEWAC>2.0.CO;2.

——, S. Zhong, W. J. Shaw, J. M. Hubbe, X. Bian, and J. Mittelstadt, 2001: Cold pools in the Columbia basin. *Wea. Forecasting*, **16**, 432–447, doi:10.1175/1520-0434(2001)016<0432:CPITCB>2.0.CO;2.

——, T. Haiden, B. Pospichal, S. Eisenbach, and R. Steinacker, 2004: Minimum temperatures, diurnal temperature ranges, and temperature inversions in limestone sinkholes of different

sizes and shapes. *J. Appl. Meteor.*, **43**, 1224–1236, doi:10.1175/1520-0450(2004)043<1224:MTDTRA>2.0.CO;2.

Wu, W., and R. E. Dickinson, 2004: Time scales of layered soil moisture memory in the context of land–atmosphere interaction. *J. Climate*, **17**, 2752–2764, doi:10.1175/1520-0442(2004)017<2752:TSOLSM>2.0.CO;2.

Xia, Y., and Coauthors, 2012: Continental-scale water and energy flux analysis and validation for the North American Land Data Assimilation System project phase 2 (NLDAS-2): 1. Intercomparison and application of model

products. *J. Geophys. Res.*, **117**, D03109, doi:10.1029/2011JD016048.

Zängl, G., 2005: Formation of extreme cold-air pools in elevated sinkholes: An idealized numerical process study. *Mon. Wea. Rev.*, **133**, 925–941, doi:10.1175/MWR2895.1.

Zhong, S. C., D. Whiteman, X. Bian, W. J. Shaw, and J. M. Hubbe, 2001: Meteorological processes affecting the evolution of a wintertime cold air pool in the Columbia basin. *Mon. Wea. Rev.*, **129**, 2600–2613, doi:10.1175/1520-0493(2001)129<2600:MPATEO>2.0.CO;2.